frontiers | Frontiers in Materials

TYPE Original Research
PUBLISHED 11 May 2023
DOI 10.3389/fmats.2023.1178475

OPEN ACCESS

EDITED BY
Yongqian Shi,
Fuzhou University, China

REVIEWED BY
Ye-Tang Pan,
Beijing Institute of Technology, China
Jun Sun,
Beijing University of Chemical Technology, China
Gang Tang,
Anhui University of Technology, China
Congling Shi,
China Academy of Safety Sciences and Technology, China

*CORRESPONDENCE
Shuang Hu,
xhl0109@outlook.com

RECEIVED 02 March 2023
ACCEPTED 26 April 2023
PUBLISHED 11 May 2023

CITATION
Hu S, Peng J, Tian J and Xiao C (2023), Thermal performance of thermoplastic polyurethane composites with microencapsulated piperazine pyrophosphate.
Front. Mater. 10:1178475.
doi: 10.3389/fmats.2023.1178475

Thermal performance of thermoplastic polyurethane composites with microencapsulated piperazine pyrophosphate

Shuang Hu*, Jianwen Peng, Jianjun Tian and Chong Xiao

ASAP Technology (Jiangxi) Co, Ltd, Ji'an, China

This study synthesized and investigated the efficacy of a novel flame retardant, melamine formaldehyde microencapsulated piperazine pyrophosphate (MFPAPP), in improving the thermal and flame-retardant properties of thermoplastic polyurethane (TPU). When TPU was incorporated with 30wt% MFPAPP, the limiting oxygen index (LOI) value of the TPU/MFPAPP composite increased to 38.8%, achieving a V-0 rating. The thermogravimetric test (TG) results confirmed that MFPAPP significantly enhanced the thermal stability of the TPU/MFPAPP composite, as indicated by the increased char residue at 800°C, which was up to 22.4wt%. Compared with the pure TPU samples, the peak heat release rate (PHRR) and total heat release (THR) of TPU/MFPAPP30 decreased by 53% and 45%, respectively. TPU/MFPAPP10 maintained a V-0 rating after the water immersion test, whereas TPU/PAPP degraded to a V-2 rating. Scanning electron microscopy (SEM), Raman spectra, and X-ray photoelectron spectroscopy analyses revealed that MFPAPP promoted the formation of heat-resistant and dense expanded carbon layers. In summary, MFPAPP demonstrated remarkable flame retardancy and thermal stability, making it an ideal candidate for enhancing the fire safety of TPU materials.

KEYWORDS

microencapsulation, piperazine pyrophosphate, thermoplastic polyurethane, thermal analysis, water immersion test

Introduction

Thermoplastic polyurethane (TPU) has a unique structure of alternating soft and hard segments, which endows it with special properties unmatched by other elastomers, including high strength, high wear resistance, aging resistance, and a wide range of hardness (Yu et al., 2019; Wang et al., 2020; Liu et al., 2021a; Luo et al., 2022). TPU is widely used in high-end fields such as military and national defense, electronic appliances, medical and healthcare applications, and sports equipment, which has become one of the fastest-growing polyurethane types (Wang et al., 2019a; Liu et al., 2019; Yu et al., 2020; Liu et al., 2021b). However, the limiting oxygen index of TPU is about 18 vol%, which is a flammable material with a great fire hazard (He et al., 2021; Xiao et al., 2021). Therefore, scholars have focused on the development of TPU materials with flame-retardant properties.

Studies have reported the flame retardancy of TPU, mainly in two ways: additive flame retardant and reactive flame retardant (Tang et al., 2020a; Tang et al., 2021a). Among them, the additive type has the advantages of a simple process, low cost, and good flame retardance (Tang et al., 2020). Additive flame retardants include halogen flame retardants, metal hydroxides, phosphorus-based flame retardants, nitrogen-containing flame retardants, and ionic liquids (Chen et al., 2017; Jiao et al., 2019; Wan et al., 2021; Ozcelik et al., 2022; Hu et al., 2023). Among additive flame retardants, phosphorus-based flame retardants are one of the most widely used ways to prepare flame-retardant TPU. Phosphorus-based flame retardants generate phosphoric acid, metaphosphoric acid, pyrophosphoric acid, and phosphorus oxide compounds during thermal decomposition. These acid compounds can promote dehydration and carbonization of the polymer matrix, thus improving the carbonization rate and enhancing the flame-retardant properties of the polymer composites (Jia et al., 2019; Yang and Shao, 2021). Zhou et al. (2019) added aluminum hypophosphite (AHP) and phosphorus tailings (PT) to TPU. The TG test results showed that the compounding of PT and AHP improved the thermal stability of TPU composites, with a significantly increased carbon residue at 800°C. The cone calorimetry test (CCT) results showed that the peak heat release rate (PHRR) and total heat release rate (THR) of the samples with AHP addition of 25wt% decreased by 89% and 68%, respectively, and the total smoke release (TSR) was reduced by 58.8% compared to pure TPU. Wang et al. (2021) compounded APP and expanded graphite (EG) and prepared TPU/APP/EG composites by microlayer co-extrusion technology. The microlayer co-extrusion technology allowed easier dispersion of APP and EG particles in the polymer matrix, as well as more uniform and better flame-retardant effects. When the addition amount was 15% APP and EG (APP: EG = 1:1), the LOI of the composite prepared by micro-layer co-extrusion technology reached 30.9 vol%. Shi et al. (2022) synthesized Co-MOF@MXene hybrid flame retardants, which were incorporated into TPU to enhance its fire retarding properties. When 2 wt% Co-MOF@MXene was added, the smoke production rate and total smoke production of TPU/Co-MOF@MXene composites decreased by 58.8% and 47.5% compared with pure TPU. Cai et al. (2022) grafted cross-linked polydimethylsiloxane (PDMS) on the surface of black phosphorus to improve the moist ambient stability and flame retardancy efficiency. PDMS-BP was further introduced to enhance the flame retardancy of the TPU composites. With only 2 wt% PDMS-BP loading, TPU/PDMS-BP showed PHRR and THR decreases of 59.6% and 14.3%, respectively, compared with pure TPU.

Generally, phosphorus-based flame retardant shows acceptable flame-retardant properties. However, pure phosphorus-based flame retardant still has challenges, including water absorption tendency, poor thermal stability, and instability in the air. The microencapsulation of flame retardants can effectively tackle these drawbacks. Zhu et al. (2020) prepared carbon black microencapsulated ammonium polyphosphate (APP@CB) by coating nano-carbon black (CB) on the surface of APP particles with triethoxysilane (APTS). Furthermore, APP@CB was added to TPU to fabricate TPU/APP@CB composites. The LOI value of the TPU composite was as high as 29 vol% for a 2 wt% CB coating. Yang et al. (2021) microencapsulated APP with glycidyl methacrylate (GMA) and prepared a series of flame-retardant rigid polyurethane composites (RPUF/GMAAPP). Their tests showed that with the same loading of GMAAPP and APP, the compressive performance of RPUF/GMAAPP improved by 5% compared with that of RPUF/APP. Cheng et al. (2021) used chitosan (CH) and chitosan/lignosulfonate (CH/LS) as the shell materials to prepare microencapsulated red phosphorus (MRP). RP@CH and RP@CH/LS were used as flame retardants for epoxy resin (EP). In the cone calorimeter test, the peak heat release rate (PHRR) of EP/7wt% RP@CH/LS was 59.7% lower than that of pure EP.

In the present study, microencapsulated piperazine pyrophosphate (MFPAPP) was prepared using melamine-formaldehyde resin, which showed a synergistic phosphorus-nitrogen flame retardant effect. MFPAPP was added to TPU to prepare TPU/MFPAPP composites, which were then subjected to various analyses to evaluate their thermal stability, combustion characteristics, pyrolysis gas products, and char residue structure. These analyses included thermogravimetry (TG), microcalorimetry (MCC), thermogravimetric infrared (TG-FTIR), and scanning electron microscopy (SEM). By investigating these parameters, the results provide both experimental and theoretical support for the development of high-performance flame retardant TPU.

Experiment

Materials

TPU (E8185) was purchased from Baoding Bangtai New Polymer Materials Co., Ltd. Melamine, formaldehyde, ethanol, and sodium carbonate were provided by Sinopharm. Deionized water was made in the laboratory.

MFPAPP preparation

First, 10 g of melamine, 17.9 mL of 37% formaldehyde aqueous solution, and 50 mL of distilled water were added to a 500-mL three-necked flask. The pH of the solution was then adjusted to 8.5 using a 10 wt% sodium carbonate solution. The temperature was raised to 80°C with stirring and then stirred for 30 min to obtain a transparent and clear melamine-formaldehyde pre-polymer for the next experiment.

A total of 60 g PAPP was dispersed in 150 mL of ethanol solution. The pre-polymer was then added to the mixture. The pH of the solution was adjusted to 3.6, and the temperature was raised to 80°C and further reacted for 2 h. The mixture was filtered, washed, and dried after cooling to room temperature. White powders were obtained after heating at 70 °C for 12 h.

Preparation of polyurethane elastomer composites

First, the TPU particles, and PAPP and MFPAPP powders were heated at 80°C for 6 h to constant weights. Then, TPU pellets were added into the mixer and mixed at 180°C for 5 min at 100 r/min until

TABLE 1 TPU and FR-TPU composition.

Sample	TPU	PAPP	MFPAPP
TPU	50	0	—
TPU/PAPP10	45	5	—
TPU/PAPP20	40	10	—
TPU/PAPP30	35	15	—
TPU/MFPAPP10	45	—	5
TPU/MFPAPP20	40	—	10
TPU/MFPAPP30	35	—	15

they melted. Then, PAPP and MFPAPP were added and mixed for 10 min. The mixed samples listing in Table 1 were hot-pressed at 10 MPa for 10 min to obtain a 3.2-mm sheet for further testing.

Measurements and characterization

An X-ray photoelectron spectroscopy (XPS) spectrometer (VG ESCALAB II) was used to detect the surface element content of PAPP and MFPAPP under the condition of Al Kα excitation radiation (hv = 1,253.6 eV) in ultra-high vacuum.

A vertical combustion (UL-94) CZF-3 type horizontal and vertical combustion tester (Nanjing Jiangning Instrument Factory) was used to test the flame-retardant properties of the composite materials according to GB/T2408-2021. The sample size was 100 mm × 10 mm × 10 mm, and five pieces were selected for each group. The burning time and the presence of dripping during the burning process were also recorded.

The limiting oxygen indexes (LOIs) of the composites were measured using a JF-3 oxygen index analyzer (Nanjing Jiangning Instrument Factory) according to ASTM D2863. The sample size was 100 mm × 10 mm × 10 mm.

Water resistance test: The samples were soaked in water for 10 and 20 days at room temperature and then dried to a constant weight for the LOI and UL-94 tests.

Scanning electron microscope (SEM)-energy spectroscopy was used to analyze the macroscopic morphology of the carbon slag after calcination in the muffle furnace at a working voltage of 10 kV.

Fourier transform infrared spectroscopy (FTIR) (Nicolet 6700 FTIR) with a wave-number range of 400–4,000 cm^{-1} was performed to test the flame-retardant powder before and after encapsulation.

Thermogravimetry (TG): The thermal stability of the samples was characterized on a Q5000 thermal analyzer. First, 5–10 mg of the samples was heated from room temperature to 700°C at 20°C/min in a nitrogen atmosphere. The TG curve and DTG curves were recorded. The temperatures corresponding to 5% and 50% weight loss were defined as the initial decomposition temperature ($T_{-5\%}$) and the midpoint temperature of weight loss ($T_{-50\%}$), respectively. The temperature corresponding to the maximum weight loss rate was defined as T_{max}.

Thermogravimetric-infrared (TG-IR) spectroscopy was performed using a TGA Q500 infrared thermogravimetric analyzer connected to a spectrophotometer (Nicolet 6700 FTIR). Approximately 5–10 mg of the sample was placed in an aluminum crucible and heated from 30°C to 700°C at 20°C/min (nitrogen atmosphere, flow rate of 70 mL/min).

Raman spectroscopy (LRS) was performed using an inVia Raman spectrometer on the carbon residue after combustion of the sample composites to analyze the graphitization degree.

The combustion characteristics of the samples were analyzed by micro combustion calorimetry (MCC, Govmark) according to the ASTM D 7309–2007a. At a nitrogen flow of 8×10^{-5} m^3 min^{-1}, 4–6 mg of samples was heated from 100°C to 650°C at 1°C/s. The volatile anaerobic pyrolysis products in the nitrogen flow were mixed with a pure oxygen flow of 8×10^{-5} m^3 min^{-1} and then placed into the combustion furnace at 900°C. Parameters such as the release rate were obtained according to the oxygen consumption.

Results and discussion

Characterization of MFPAPP

Figure 1 shows the SEM images of PAPP and MFPAPP. In Figure 1A, PAPP shows particle sizes of 0.1–20 μm with irregular shapes and rough surface structures. Figure 1B shows the morphology of MFPAPP, which was composed of ball-like structures with significantly larger particle sizes and small particles on the surface. Comparisons showed significant changes in the MFPAPP surface structure, which was ascribed to melamine–formaldehyde wrapping on the surface of PAPP particles, suggesting successful MFPAPP fabrication.

X-ray photoelectron spectroscopy (XPS) is an effective method to analyze the chemical composition and bonding state of a material's surface. Figure 2 shows the XPS spectra of MFPAPP and PAPP. The corresponding data are listed in Table 2. The P_{2p} and P_{2s} peak vibrations occurred at 135 eV and 192 eV, respectively. The peaks at around 285 eV and 398 eV could be ascribed to C_{1s} and N_{1s}, respectively. As shown in Figure 2, PAPP exhibited C of 44.34%, C of 35.52%, N of 10.19, and P of 9.95%. In contrast, MFPAPP exhibited a significantly increased N of 33.08% due to the high N content in MF resin, suggesting the successful fabrication of MFPAPP. Furthermore, the P content in MFPAPP decreased to 5.20%, indicating encapsulation of the PAPP particles by the MF resin.

Thermal stability of the composites

Figure 3 shows the TG and DTG curves of TPU and the FR-TPU composites under nitrogen conditions. The corresponding data are listed in Table 3. The TPU decomposition was divided into two stages. First, TPU started to decompose at 328°C and then quickly reached the first thermal weight loss peak. This stage was mainly ascribed to the hard segment degradation of TPU molecular chains (Zhou et al., 2016). TPU pyrolysis reached the second peak at around 428°C. At this stage, the polyol segment in TPU molecular chain began to break to form a multi-molecular mixture. The char residue was 2.4wt% when the temperature reached 800°C. With the addition of PAPP and MFPAPP, the $T_{-5\%}$ of the FR-TPU composites was lower. The $T_{-5\%}$ value of TPU/

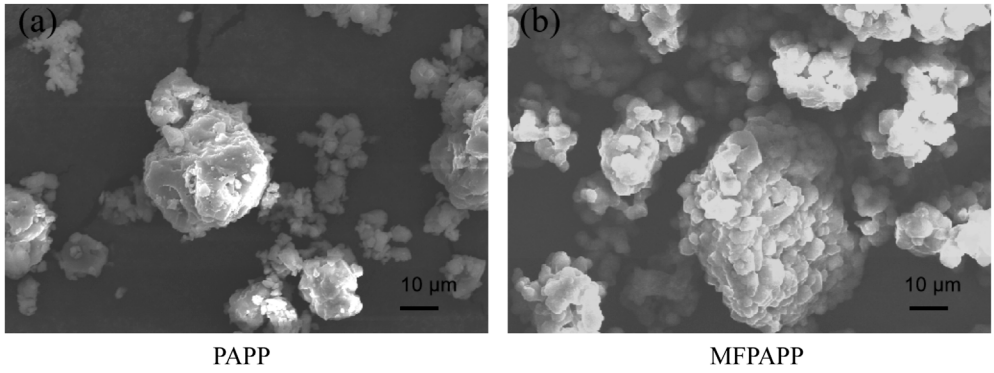

FIGURE 1
SEM images of PAPP and MFPAPP. **(A)** PAPP and **(B)** MFPAPP.

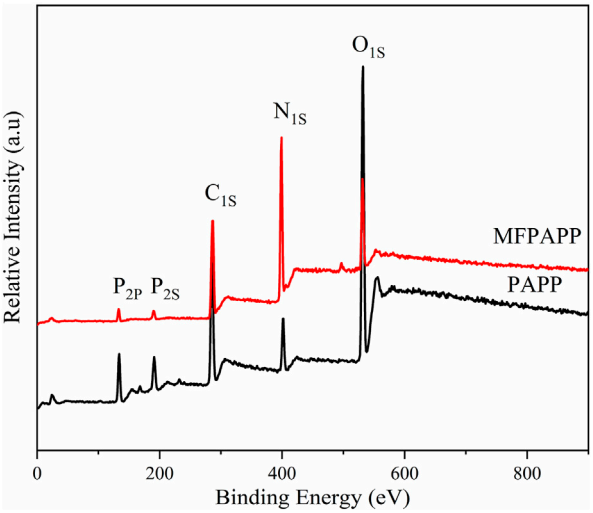

FIGURE 2
XPS spectra of MFPAPP and PAPP.

TABLE 2 XPS test results for PAPP and MFPAPP.

	C (at%)	O (at%)	N (at%)	P (at%)
PAPP	44.34	35.52	10.19	9.95
MFPAPP	40.06	21.66	33.08	5.20

MFPAPP composites decreased with increasing MFPAPP loading, possibly because the MF resin promoted the reaction between PAPP and the polyurethane molecular chain at this stage, thus promoting the premature degradation of TPU molecular chains. The T_{max1} and T_{max2} values of FR-TPU composites were higher than those of pure TPU, possibly because the phosphate and polyphosphate decomposed by PAPP and MFPAPP promoted the decomposition of the TPU matrix and formed a stable char layer. At 800°C, the char residue of TPU/PAPP10 was 13.7wt%, compared with 15.5wt% for TPU/MFPAPP10. A comparison of the aforementioned data showed that MFPAPP possessed higher char residues, which may be attributed to a synergistic effect between MF and PAPP to promote char residue formation, thereby protecting the fundamental material (Gao et al., 2022).

Combustion properties of the FR-TPU composites

Microcalorimetry (MCC) is an effective method for evaluating the fire performance of composite materials and requires only milligrams of samples (Xiao et al., 2017). Figure 4 shows the heat release rate (HRR) curves for TPU and the FR-TPU composites from the MCC tests. The results are listed in Table 4. In Figure 4, pure TPU shows two peak heat release rate (PHRR), with the second PHRR as high as 394 W/g, significantly higher than the first one. The total heat release (THR) reached 25.4 kJ/g at the end of combustion. With the addition of PAPP, the PHRR values of TPU/PAPP composites decreased with increasing PAPP loading. When MFPAPP replaced PAPP, the first PHRR value of TPU/MFPAPP composites was smaller and the second peak was larger than those for TPU/PAPP, consistent with the promotion of TPU decomposition by MF gas. The T_{PHRR} value confirmed this conjecture. When the MF decomposition ended, the PAPP decomposition formed phosphoric and pyrophosphoric acids, promoted the carbonization process of the TPU matrix, and prevented flame spread. The THR value of TPU/MFPAPP30 was 45% lower than that of the pure sample, indicating that MFPAPP improved the fire resistance of the composites.

Table 5 shows the limiting oxygen index (LOI) and vertical combustion (UL-94) test grades for TPU and the FR-TPU composites. The pure TPU without flame retardant shows a low LOI value of 22.9 vol% and no rating in the UL-94 test. It melted, deformed, and expanded the burning area after ignition, which is extremely dangerous in a fire. When PAPP was added, the LOI value of FR-PAPP composites increased significantly with the increasing addition of the flame retardant. When the additional amount of flame retardant was 30 wt%, the LOI values of TPU/PAPP30 and TPU/MFPAPP30 were 38.6% and 38.8%, respectively, which also

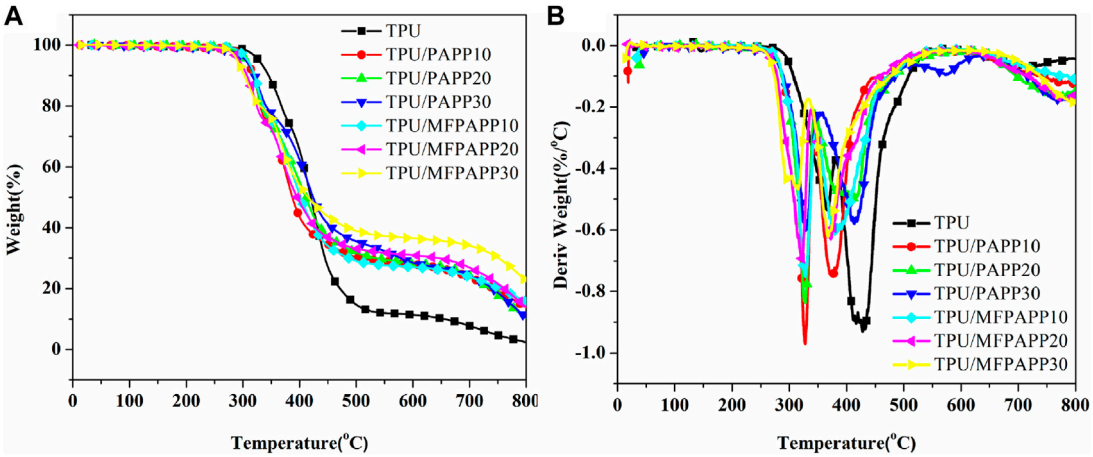

FIGURE 3
(A) TG and **(B)** DTG curves of TPU and FR-TPU composites.

TABLE 3 Thermogravimetric data for the TPU and FR-TPU composites.

Sample	$T_{-5\%}$/°C	T_{max1}/°C	T_{max2}/°C	Char residue at 800 C/wt%
TPU	328	365	428	2.4
TPU/PAPP10	305	328	371	13.7
TPU/PAPP20	305	326	405	10.3
TPU/PAPP30	304	327	412	10.5
TPU/MFPAPP10	308	326	380	15.5
TPU/MFPAPP20	293	321	370	13.8
TPU/MFPAPP30	290	315	367	22.4

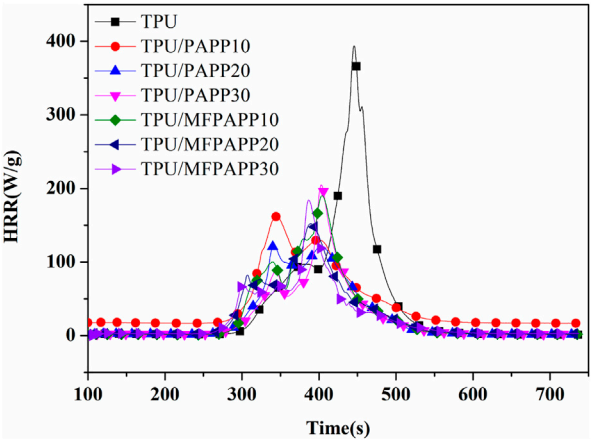

FIGURE 4
Heat release rate curves of TPU and FR-TPU from MCC.

TABLE 4 MCC test results of TPU and FR-TPU composites.

Sample	PHRR (W/g)	THR (KJ/g)	T_{PHRR} (°C)
TPU	394	25.4	445
TPU/PAPP10	161/130	16.4	345/400
TPU/PAPP20	123/121	15.2	342/403
TPU/PAPP30	87/205	14.1	343/403
TPU/MFPAPP10	100/190	17.3	340/404
TPU/MFPAPP20	82/152	15.5	307/389
TPU/MFPAPP30	69/184	14.0	301/386

Flame retardant performance of TPU and FR-TPU.

successfully passed the UL-94 V-0 rating. In addition, with the same loading of flame retardant, the TPU/MFPAPP composites showed higher LOI values than their counterparts with PAPP loading, confirming that MFPAPP showed better flame-retardant performance than TPU. This phenomenon was attributed to the synergistic effect between the MF resin and PAPP.

Flame retardant experiments of the FR-TPU composites were also conducted after water immersion experiments (Table 6. A deterioration in the flame-retardant properties of TPU was

TABLE 5 LOI test results of TPU and FR-TPU composites after immersion in water.

Sample	Pure (vol%)	10 days (vol%)	20 days (vol%)
TPU	22.9	22.5	22.0
TPU/PAPP10	30.2	28.3	27.5
TPU/PAPP20	32.8	31.4	30.3
TPU/PAPP30	38.6	31.6	31.0
TPU/MFPAPP10	31.1	30.8	29.9
TPU/MFPAPP20	33.4	32.8	32.2
TPU/MFPAPP30	38.8	34.4	34.3

TABLE 6 UL-94 test results of TPU and FR-TPU composites after immersion in water.

Sample	Pure	10 days	20 days
TPU	NR	NR	NR
TPU/PAPP10	V-0	V-2	V-2
TPU/PAPP20	V-0	V-0	V-0
TPU/PAPP30	V-0	V-0	V-0
TPU/MFPAPP10	V-0	V-0	V-0
TPU/MFPAPP20	V-0	V-0	V-0
TPU/MFPAPP30	V-0	V-0	V-0

observed after immersion in water. After 10 days of immersion, the LOI value was 22.5 vol%. After 20 days of immersion, the value further decreased to 22.0 vol%. A similar phenomenon was also observed in the TPU/PAPP composites. TPU/PAPP10 showed decreased LOI values of 28.3 vol% and 27.5 vol% after water immersion for 10 and 20 days, confirming the decreased flame retardancy of TPU/PAPP10, which was ascribed to the poor water resistance of PAPP particles. Compared with TPU/PAPP10, TPU/MFPAPP10 exhibited a lower deterioration of flame retardancy, which was ascribed to the protective effect of the MF shell on PAPP particles. The shell structure may inhibit the dissolution effect of water on PAPP particles, thus maintaining the excellent flame retardancy of the TPU/MFPAPP composites (Tang et al., 2020b).

To further understand the gas-phase products of FR-TPU composites during pyrolysis, TG-FTIR was conducted. Figure 5 provides a three-dimensional view of the gas-phase products of TPU and the TPU/PAPP30, and TPU/MFPAPP30 composites. After adding PAPP and MFPAPP, the decomposition products of the TPU composites were similar and mainly distributed at 3,800–3,700 cm^{-1}, 2,500–2,300 cm^{-1}, 1800–1700 cm^{-1}, 1,600–1,500 cm^{-1}, and 700–600 cm^{-1} (Liu et al., 2022a).

Figure 6 shows the typical gas-phase product release intensity *versus* time during the pyrolysis of TPU, TPU/PAPP30, and TPU/MFPAPP30. The Gram–Schmidt curves (Figure 6A) showed that TPU, TPU/PAPP30, and TPU/MFPAPP30 had two gas evolution

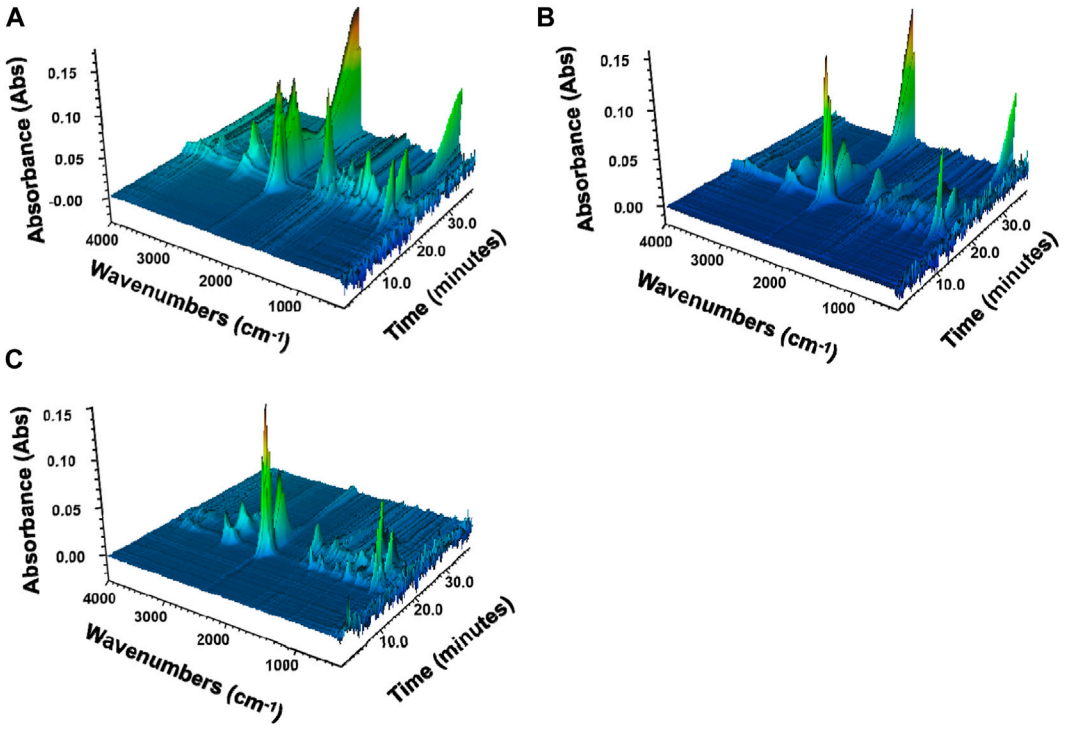

FIGURE 5
3D-FTIR spectra of **(A)** TPU, **(B)** TPU/PAPP30, and **(C)** TPU/MFPAPP30.

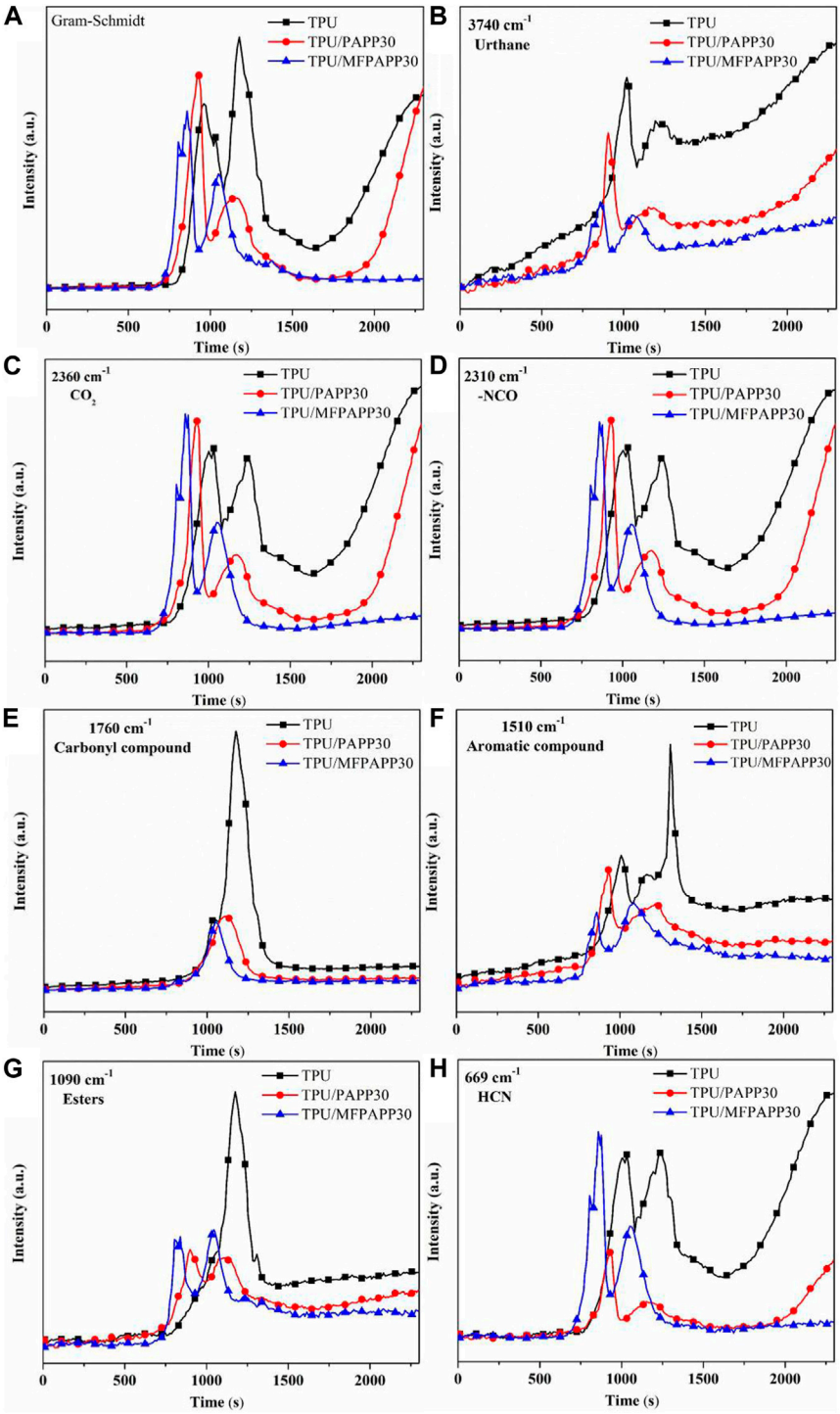

FIGURE 6
Comparisons of the gas-phase product intensities of TPU, TPU/PAPP30, and TPU/MFPAPP30. **(A)**Gram–Schmidt; **(B)** urethane; **(C)** CO_2; **(D)** NCO; **(E)** carbonyl compound; **(F)** aromatic compound; **(G)** esters; **(H)** HCN.

processes, corresponding to two decomposition stages of polyurethane molecular chains, consistent with the thermogravimetric results. Meanwhile, the peak intensity of TPU/PAPP30 and TPU/MFPAPP30 in the first decomposition stage was higher than that of TPU, indicating that PAPP and MFPAPP promoted the degradation of polyurethane hard segment chains into isocyanate compounds, amines, hydrocarbons, and CO_2 (Wu et al., 2019). Figure 6 b), e), f), g) shows the release intensities of urethanes, carbonyls, aromatics, and esters, respectively. This release intensity was lower than that of pure TPU. Figure 6 c), d), h) provides the intensities for CO_2, isocyanate, and HCN, all of which are lower than those of untreated TPU. Among them, isocyanate and

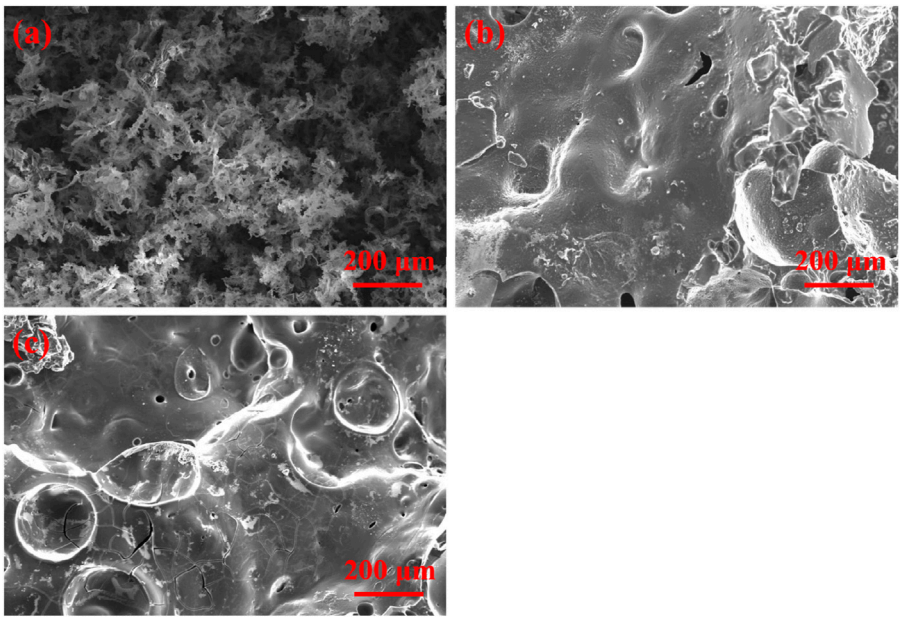

FIGURE 7
SEM photographs of carbon residues in TPU **(A)**, TPU/PAPP30 **(B),** and TPU/MFPAPP30 **(C)**.

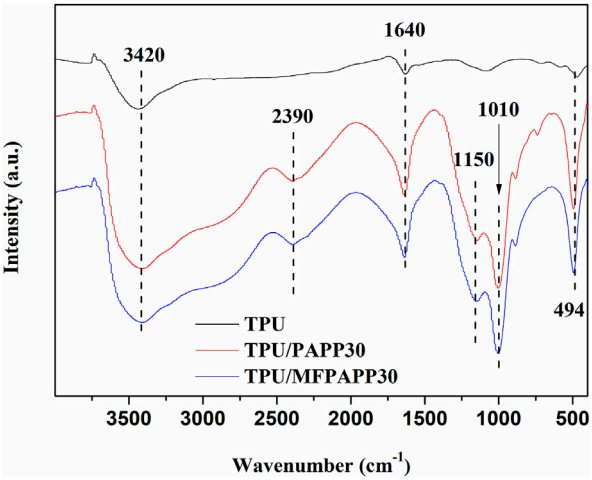

FIGURE 8
FTIR spectra of carbon residues for TPU, TPU/PAPP30, and TPU/MFPAPP30.

CO_2 were typical gaseous products in the first degradation stage. Their reduction occurred due to the excellent catalytic carbonization effects of PAPP and MFPAPP, which promoted the gas-phase products generated by the cracking of polyurethane molecular chains into the condensed phase. Additionally, CO_2 and water generated by the pyrolysis of PAPP and MFPAPP can play a role in diluting the combustible gas. Moreover, PAPP and MFPAPP can act as free radical scavengers during combustion, capturing the reactive H and HO radicals, thereby interrupting the combustion reaction (Chen et al., 2022). HCN is a toxic product of TPU pyrolysis, which can cause casualties in a fire. Figure h) shows that the HCN intensity of TPU/PAPP30 was greatly reduced compared with pure TPU, implying that the addition of PAPP can improve the fire safety of TPU composites.

Carbon layer analysis

Figure 7 shows SEM images of the char slag after calcination of the composites in the muffle furnace. Figure 7A confirms that the carbon slag of pure TPU is loose and fragile and easily falls apart; thus, it cannot play a role as a condensed-phase flame retardant. Compared with TPU, the carbon residue of TPU/PAPP30 was more complete. Although some holes were observed, the overall compactness was greatly improved, indicating that pyrophosphate and polyphosphate pyrolyzed by PAPP promoted the carbonization process of the TPU matrix. Figure 7C shows the carbon residues of TPU/MFPAPP30, in which the hole structures have almost disappeared, and the compactness of the char layer is also enhanced, possibly due to the combined action of MF and PAPP to promote the carbonization of the TPU matrix, which further improved the compactness of the carbon layer. The enhanced carbon layer was conducive to improving the fire-retardant performance of the composites. This phenomenon was highly consistent with the results of flame retardant tests (Tang et al., 2021b).

Figure 8 shows the FTIR spectra of the carbon residues in TPU, TPU/PAPP30, and TPU/MFPAPP30. The characteristic peaks of the carbon residues are very different, in which 3,420 cm^{-1} corresponds to the O-H stretching vibration (Chen et al., 2019), and 1,640 cm^{-1} is the characteristic peak of the C=C bond. The TPU/PAPP and TPU/MFPAPP composites showed a new absorption peak, in which

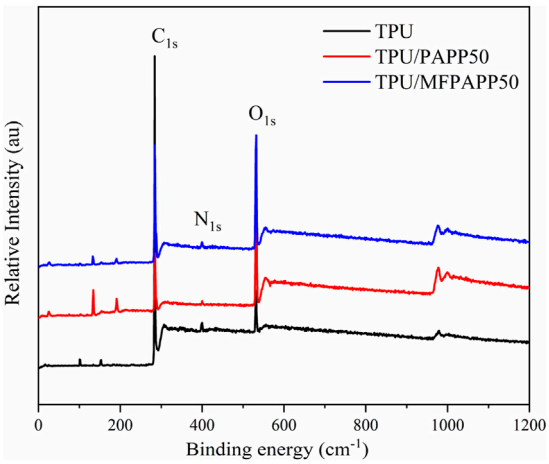

FIGURE 9
XPS spectra of carbon residues for TPU, TPU/PAPP30, and TPU/MFPAPP30.

TABLE 7 XPS results of carbon residues for TPU, TPU/PAPP30, and TPU/MFPAPP30 XPS.

Sample	C	N	O	P
TPU	88.2	3.73	8.07	—
TPU/PAPP30	42.11	2.22	45.88	9.79
TPU/MFPAPP30	66.13	3.19	27.79	2.89

3,290 cm^{-1} corresponded to the stretching vibration of the P-OH group (Hu et al., 2020) and 1,150 cm^{-1} and 1,010 cm^{-1} were attributed to the P=O and P-O-P bonds, respectively (Zhu et al., 2018). PAPP and MFPAPP promoted the formation of C=C from polyurethane molecular chains, which benefitted the formation of a compact carbon layer. Additionally, the introduction of phosphate into the carbon layer further improved the heat resistance of the composites.

To further understand the main elements in the carbon residue and their binding states, XPS tests were performed (Figure 9 and Table 7. The carbon residues of TPU mainly contained C, N, and O. After adding PAPP and MFPAPP, the C and N contents of the carbon residues in TPU/PAPP30 and TPU/MFPAPP30 decreased, while the content of O increased. The P element was also observed, which was ascribed to the phosphate decomposed by PAPP, which participated in the formation of the char layer.

Furthermore, the main elements C, N, and O in the carbon residue were peak fitted using XPS PEAK41 software to understand the binding state (Table 6). Figure 10 shows the C (1s) peak-fitted spectra of carbon residues in TPU and TPU/PAPP composites. The corresponding data are listed in Table 8. The peak at 284.7 eV represented the C element in C-C or C-H bonds, which corresponded to the graphitic carbon structure in the carbon residue. The peak at 285.7 eV represented the C element as C-O or C-N bonds, mainly corresponding to the structures of esters, ethers, alcohols, and phenols on the surface of the carbon layer. The peak at 287.4 eV represented C as C=O or C=N, corresponding to carbonyl groups, carboxylic acid (salt), ester groups, aromatic heterocyclic compounds, etc. on the surface of the carbon layer (Wu et al., 2019). The amounts of C-C/C-H, C-O/C-N, and C=O/C=N in TPU were 61.05%, 35.65%, and 3.30%, respectively. After adding PAPP, the C-O/C-N content of TPU/PAPP30 increased significantly. In TPU/MFPAPP30, the C-C/H content was increased significantly, indicating that MFPAPP enhanced the compactness of the carbon residues.

Figure 11 shows the O_{1s} peak-fitted spectra of the carbon residues in the TPU composites. The corresponding data are list in Table 9. The peak at 531.3 eV corresponded to the =O structure in the form of carbonyl, quinone, carboxylic acid (salt), and ester in the carbon residues, The peak at 532.5 eV corresponded to the O element in the form of alcohol, ether, and phenol, while the peak at 533.7 eV corresponded to the adsorbed oxygen (O_2) and free water (Tang et al., 2020c). The contents of = O, -O-, and O_2/H_2O in the carbon residues of TPU accounted for 28.75%, 44.35%, and 26.90%, respectively. After adding PAPP, the -O- structure in the carbon residues of TPU/PAPP30 increased to 51.43%, while the content of the O_2/H_2O structure did not change obviously. When MFPAPP was added, the content of the =O structure in the carbon residue of TPU/MFPAPP30 decreased slightly, while the content of the O element in the form of -O- increased to 62.33%. This phenomenon suggested significant improvement in the compactness of the carbon residue, consistent with the SEM test findings.

Figure 12 shows the N_{1s} peak-fitted spectra of carbon residues for the TPU composites. The corresponding data are listed in Table 10. The peak at 398.8 eV was attributed to the N element in the amide and amine compounds with the -NH- structure in the carbon residue, while the peak at 400.4 eV could be ascribed to the N element in aromatic heterocyclic compounds with the = N structure (Chen et al., 2021). PAPP or MFPAPP promoted the formation of the = N structure in the carbon residue, which benefitted the formation of aromatic heterocycles and enhanced the fire resistance of the carbon residue.

Figure 13 shows the Raman spectra of the carbon residues for the TPU composites to investigate the effect of PAPP and MFPAPP on the carbonization of TPU composites in fire. All the curves show two characteristic peaks, corresponding to the D peak (1,360 cm^{-1}) of the SP^3 vibration of amorphous carbon and the G peak (1,580 cm^{-1}) of the SP^2 vibration with a fully graphitized structure, respectively (Bernhard et al., 2016; Wang et al., 2019b). The graphitization degree of the carbon material is represented by the area ratio (I_D/I_G) of the D and G peaks (Wang et al., 2019c). The smaller the I_D/I_G, the higher the graphitization degree of the formed carbon residue and the better the fire resistance of the carbon residue (Zhu et al., 2022). I_D/I_G of pure TPU was 2.25, while that of TPU/PAPP30 decreased to 2.08 when 30 wt% PAPP was added. This mainly occurred because PAPP contained a piperazine structure, which was a good carbon source. However, phosphates and polyphosphates generated by the pyrolysis of PAPP promoted the formation of carbon layers with high degrees of graphitization in combustion. When 30 wt% MFPAPP was added, the I_D/I_G of TPU/MFPAPP30 further decreased to 2.01, confirming that the combination of MF and PAPP synergistically promoted the formation of the graphitized carbon layer and endowing TPU/MFPAPP composites with better fire retarding.

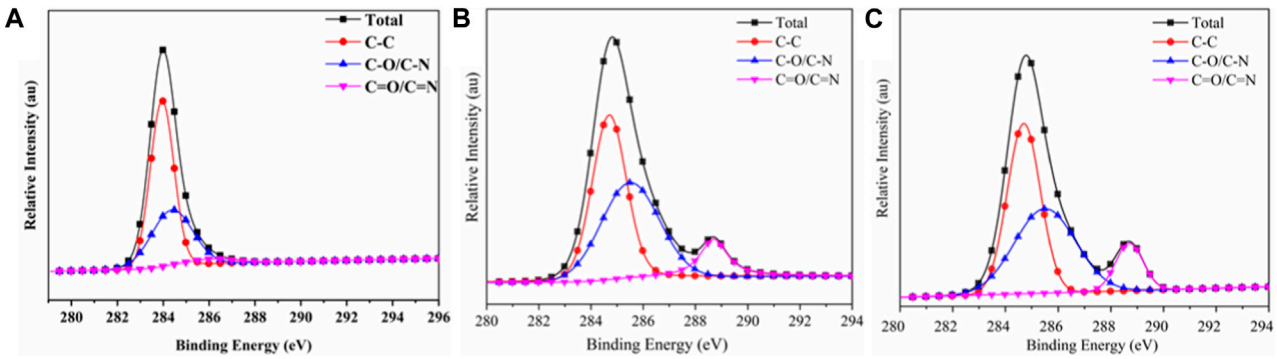

FIGURE 10
C1s spectra of carbon residues for **(A)** TPU, **(B)** TPU/PAPP30, and **(C)** TPU/MFPAPP30.

TABLE 8 Binding state of the C element in the carbon residues of TPU and FR-TPU composites.

Sample	C-C/C-H	C-O/C-N	C=O/C=N
	284.7 eV (%)	285.7eV (%)	287.4eV (%)
TPU	61.05	35.65	3.30
TPU/PAPP30	46.13	42.60	11.27
TPU/MFPAPP30	46.56	42.54	10.00

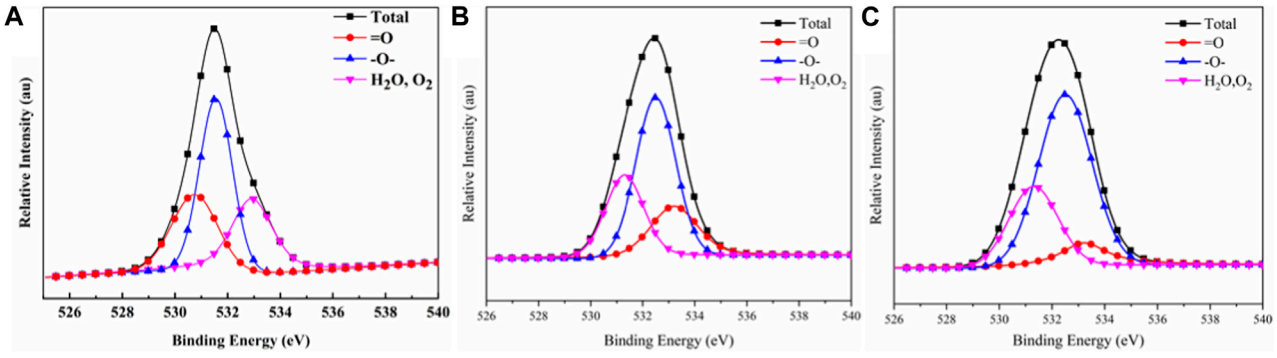

FIGURE 11
O1s spectra of the carbonr esidues in **(A)** TPU, **(B)** TPU/PAPP30, and **(C)** TPU/MFPAPP30.

TABLE 9 Binding states of the O element in the carbon residues of TPU and FR-TPU composites.

Sample	= O	-O-532.5 eV (%)	O_2/H_2O
	531.3 eV (%)		533.2 eV (%)
TPU	28.75	44.35	26.90
TPU/PAPP30	21.25	51.43	27.32
TPU/MFPAPP30	10.69	62.33	26.98

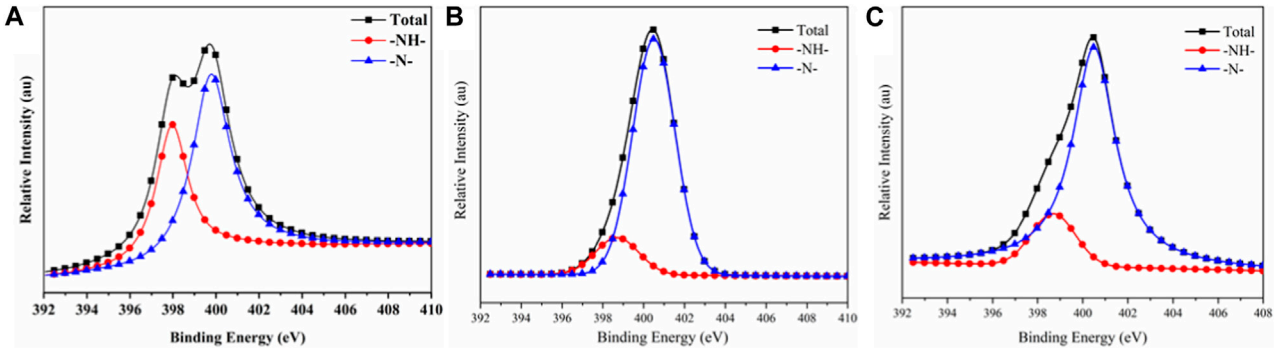

FIGURE 12
Carbon residue N1s spectra of **(A)** TPU, **(B)** TPU/PAPP30, and **(C)** TPU/MFPAPP30.

TABLE 10 Binding state of N element in the carbon residues of TPU and FR-TPU composite materials.

Sample	-NH	= N
	398.7 eV (%)	400.4 eV (%)
TPU	40.93	59.07
TPU/PAPP30	13.83	86.17
TPU/MFPAPP30	13.96	86.04

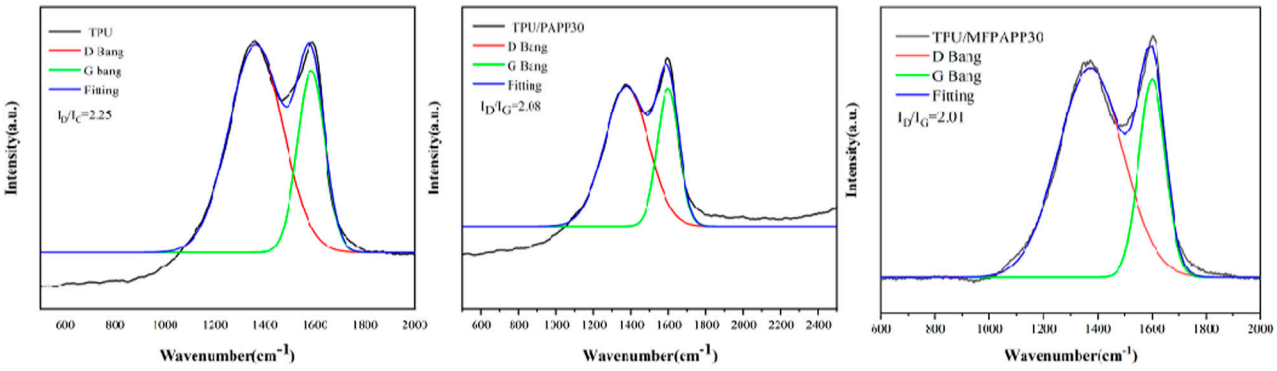

FIGURE 13
Raman spectra of carbon residues for TPU and FR-TPU composites.

Conclusion

This study fabricated microencapsulated piperazine pyrophosphate by a simple method using melamine formaldehyde resin as the shell material. The effects of piperazine pyrophosphate (PAPP) and melamine formaldehyde resin microencapsulated piperazine pyrophosphate (MFPAPP) on the flame-retardant properties of thermoplastic polyurethane (TPU) were investigated. The thermogravimetric (TG) test showed that MFPAPP promoted the early decomposition of the TPU matrix and increased the carbon residue. At 800°C, the carbon residue of TPU/MFPAPP30 was as high as 22.4 wt%, which was 89% higher than that of unmodified TPU. The results of the flame-retardant test indicated that MFPAPP endowed TPU composites with excellent fire performance, with an LOI of 31.1 vol% and a UL-94 V-0 rating when 10 wt% MFPAPP was loaded, which was better than those for TPU/PAPP10. After the water immersion test, TPU/MFPAPP showed a smaller deterioration in flame retardancy compared with TPU/PAPP, which was ascribed to protection by the melamine formaldehyde resin

shell. The results of the MCC test implied that MFPAPP effectively reduced the thermal hazard caused by combustion, with significantly decreased PHRR and THR values. Compared with pure samples, the PHRR and THR values of TPU/MFPAPP30 were reduced by 53% and 45%, respectively. XPS testing of the carbon residues showed that MFPAPP promoted the TPU matrix to form carbonyl, carboxylic acid (salt), ester, aromatic heterocyclic compounds, etc., which helped form a compact carbon layer and block flame and heat transfer. This study provided a novel strategy for fabricating flame-retardant TPU composites with excellent fire performance and water resistance.

Data availability statement

The original contributions presented in the study are included in the article/Supplementary Material. Further inquiries can be directed to the corresponding author.

Author contributions

SH: conceptualization, methodology, and formal Analysis. JP: data curation and investigation. JT: resources and supervision. CX: validation and visualization. All authors contributed to the article and approved the submitted version.

Funding

This research was supported by the Postdoctoral Science Foundation of China (2020M671958).

Conflict of interest

Authors SH, JP, JT, and CX were employed by ASAP Technology (Jiangxi) Co., Ltd.

Publisher's note

All claims expressed in this article are solely those of the authors and do not necessarily represent those of their affiliated organizations, or those of the publisher, the editors, and the reviewers. Any product that may be evaluated in this article, or claim that may be made by its manufacturer, is not guaranteed or endorsed by the publisher.

References

Bernhard, S., Charles, A. W., and Giovanni, C. (2016). Recommendations on the scientific approach to polymer flame retardancy: Part 2—concepts. *J. Fire Sci.* 35, 3–20. doi:10.1177/0734904116675370

Cai, W., Mu, X. W., Li, Z. X., Hu, W., and Hu, Y. (2022). Poly(dimethyl siloxane)-grafted black phosphorus nanosheets as filler to enhance moisture-resistance and flame-retardancy of thermoplastic polyurethane. *Mat. Chem. Phys.* 286, 126189. doi:10.1016/j.matchemphys.2022.126189

Chen, T., Xiao, X., Wang, J., and Guo, N. (2019). Fire, thermal and mechanical properties of TPE composites with systems containing piperazine pyrophosphate (PAPP), melamine phosphate (MPP) and titanium dioxide(TiO_2). *Plast. Rubber Compos.* 48 (4), 149–159. doi:10.1080/14658011.2019.1582200

Chen, X. L., Wang, K., Li, X. X., and Jiao, C. (2021). Effects of flame retardants integrated with citrate and ammonium polyphosphate on thermal stability and flame retardancy of thermoplastic polyurethane elastomer. *Polym. Advan. Technol.* 32 (8), 2866–2878. doi:10.1002/pat.5296

Chen, X. L., Wang, Y., and Jiao, C. M. (2017). Influence of TiO_2 particles and APP on combustion behavior and mechanical properties of flame-retardant thermoplastic polyurethane. *J. Therm. Anal. Calorim.* 132 (1), 251–261. doi:10.1007/s10973-017-6847-6

Chen, H., Xia, W., Wang, N., Liu, Y., Fan, P. H., Wang, S., et al. (2022). Flame retardancy of biodegradable polylactic acid with piperazine pyrophosphate and melamine cyanurate as flame retardant. *J. Fire Sci.* 40 (4), 254–273. doi:10.1177/07349041221093546

Cheng, C., Yan, J., Lu, Y., Ma, W., Li, C., and Du, S. (2021). Effect of chitosan/lignosulfonate microencapsulated red phosphorus on fire performance of epoxy resin. *Thermochim. Acta*, 700, 178931. doi:10.1016/j.tca.2021.178931

Gao, B. B., Shi, T., Yang, X., and Zhang, S. (2022). Online formation of epoxy resin multi-hierarchical char layer to improve mass and heat barrier performance via designable "heterogeneous char-forming agent". *Compos. Part B-Eng.* 246, 110145. doi:10.1016/j.compositesb.2022.110145

He, M., Gu, K., Wang, Y., Li, Z., Shen, Z., Liu, S., et al. (2021). Development of high-performance thermoplastic composites based on polyurethane and ground tire rubber by *in-situ* synthesis. *Resour. Conserv. Recy* 173, 105713. doi:10.1016/j.resconrec.2021.105713

Hu, W. J., Li, Y. M., Pang, Y. Y., and Wang, D. Y. (2023). The preparation of phosphorus and nitrogen-containing structure towards the enhancement of flame retardancy for thermoplastic polyurethane elastomer. *Colloid Surf. A* 656, 130375. doi:10.1016/j.colsurfa.2022.130375

Hu, Z., Zhong, Z. Q., and Gong, X. D. (2020). Flame retardancy, thermal properties, and combustion behaviors of intumescent flame-retardant polypropylene containing (poly) piperazine pyrophosphate and melamine polyphosphate. *Polym. Advan. Technol.* 31 (11), 2701–2710. doi:10.1002/pat.4996

Jia, D., Guo, X., He, J., and Yang, R. (2019). An anti-melt dripping, high char yield and flame-retardant polyether rigid polyurethane foam. *Polym. Degrad. Stab.* 167, 189–200. doi:10.1016/j.polymdegradstab.2019.07.007

Jiao, C. M., Jiang, H. Z., and Chen, X. L. (2019). Properties of fire agent integrated with molecular sieve and tetrafluoroborate ionic liquid in thermoplastic polyurethane elastomer. *Polym. Advan. Technol.* 30 (8), 2159–2167. doi:10.1002/pat.4622

Liu, C., Yao, A., Chen, K., Shi, Y., Feng, Y., Zhang, P., et al. (2021). MXene based core-shell flame retardant towards reducing fire hazards of thermoplastic polyurethane. *Compos. Part B* 226, 109363. doi:10.1016/j.compositesb.2021.109363

Liu, L., Xu, Y., Li, S., Xu, M., He, Y., Shi, Z., et al. (2019). A novel strategy for simultaneously improving the fire safety, water resistance and compatibility of thermoplastic polyurethane composites through the construction of biomimetic hydrophobic structure of intumescent flame retardant synergistic system. *Compos Part B- Eng.* 176, 107218. doi:10.1016/j.compositesb.2019.107218

Liu, M., Liu, X., Sun, P., Tang, G., Yang, Y., Kan, Y., et al. (2022). Thermoplastic polyurethane composites based on aluminum hypophosphite/modified iron tailings system with outstanding fire performance. *J. Appl. Polym.Sci.* 139 (27), e52486. doi:10.1002/app.52486

Liu, X., Ge, X., Liu, M., Zhou, K., Zhu, Q., Chen, D., et al. (2021). Facile fabrication of NiAl-LDH and its application in TPU nanocomposites targets for reducing fire hazards. *Plast. Rubber Compos* 50 (6), 285–298. doi:10.1080/14658011.2021.1890515

Luo, Y., Xie, Y. H., Geng, W., Dai, G., Sheng, X., Xie, D., et al. (2022). Fabrication of thermoplastic polyurethane with functionalized MXene towards high mechanical strength, flame-retardant, and smoke suppression properties. *J. Colloid.Interf.Sci* 606, 223–235. doi:10.1016/j.jcis.2021.08.025

Ozcelik, G., Elcin, O., Guney, S., Erdem, A., Hacioglu, F., and Dogan, M. (2022). Flame-retardant features of various boron compounds in thermoplastic polyurethane and performance comparison with aluminum trihydroxide and magnesium hydroxide. *Fire. Mat.* 46 (7), 1020–1033. doi:10.1002/fam.3050

Shi, C. L., Wan, M., Hou, Z. B., Qian, X., Che, H., Qin, Y., et al. (2022). Co-MOF@MXene hybrids flame retardants for enhancing the fire safety of thermoplastic polyurethanes. *Polym. Degrad. Stabil.* 204, 110119. doi:10.1016/j.polymdegradstab.2022.110119

Tang, G., Jiang, H. H., Yang, Y. D., Chen, D., Liu, C., Zhang, P., et al. (2020). Preparation of melamine-formaldehyde resin-microencapsulated ammonium polyphosphate and its application in flame retardant rigid polyurethane foam composites. *J. Polym. Res.* 27, 375. doi:10.1007/s10965-020-02343-7

Tang, G., Liu, M., Deng, D., Zhao, R., Liu, X., Yang, Y., et al. (2021). Phosphorus-containing soybean oil-derived polyols for flame-retardant and smoke-suppressant rigid polyurethane foams. *Polym. Degr.* 191, 109701. doi:10.1016/j.polymdegradstab.2021.109701

Tang, G., Liu, X., Zhou, L., Zhang, P., Deng, D., and Jiang, H. (2020). Steel slag waste combined with melamine pyrophosphate as a flame retardant for rigid polyurethane foams. *Adv. Powder Technol.* 31 (1), 279–286. doi:10.1016/j.apt.2019.10.020

Tang, G., Zhao, R. Q., Deng, D., Yang, Y., Chen, D., Zhang, B., et al. (2021). Self-extinguishing and transparent epoxy resin modified by a phosphine oxide-containing bio-based derivative. *Front. Chem. Sci. Eng.* 15, 1269–1280. doi:10.1007/s11705-021-2042-1

Tang, G., Zhou, L., Zhang, P., Han, Z. Q., Chen, D. P., Liu, X., et al. (2020). Effect of aluminum diethylphosphinate on flame retardant and thermal properties of rigid polyurethane foam composites. *J. Therm. Anal. Calorim.* 140, 625–636. doi:10.1007/s10973-019-08897-z

Tang, G., Liu, X. L., Yang, Y. D., Chen, D., Zhang, H., Zhou, L., et al. (2020). Phosphorus-containing silane modified steel slag waste to reduce fire hazards of rigid polyurethane foams. *Adv. Powder Technol.* 31 (4), 1420–1430. doi:10.1016/j.apt.2020.01.019

Wan, L., Deng, C., Chen, H., Zhao, Z. Y., Huang, S. C., Wei, W. C., et al. (2021). Flame-retarded thermoplastic polyurethane elastomer: From organic materials to nanocomposites and new prospects. *Chem. Eng. J.* 417, 129314. doi:10.1016/j.cej.2021.129314

Wang, H. W., Qiao, H., Guo, J., Sun, J., Li, H., Zhang, S., et al. (2020). Preparation of cobalt-based metal organic framework and its application as synergistic flame retardant in thermoplastic polyurethane (TPU). *Compos. Part B-Eng.* 182, 107498. doi:10.1016/j.compositesb.2019.107498

Wang, J., Zhang, D., Zhang, Y., Cai, W., Yao, C., Hu, Y., et al. (2019). Construction of multifunctional boron nitride nanosheet towards reducing toxic volatiles (CO and HCN) generation and fire hazard of thermoplastic polyurethane. *J. Hazard. Mater* 362, 482–494. doi:10.1016/j.jhazmat.2018.09.009

Wang, L., Tawiah, B., Shi, Y., Cai, S., Rao, X., Liu, C., et al. (2019). Highly effective flame-retardant rigid polyurethane foams: Fabrication and applications in inhibition of coal combustion. *Polymers*, 11: 1776. doi:10.3390/polym11111776

Wang, S., Gao, R., and Zhou, K. (2019). The influence of cerium dioxide functionalized reduced graphene oxide on reducing fire hazards of thermoplastic polyurethane nanocomposites. *J. Colloid Interf. Sci.* 536, 127–134. doi:10.1016/j.jcis.2018.10.052

Wang, S., Shi, M., Yang, W., Yan, H., Zhang, C., An, Y., et al. (2021). Experimental investigation of flame retardancy and mechanical properties of APP/EG/TPU multilayer composites prepared by microlayer coextrusion technology. *J.Appl. Polym. Sci.* 138 (15), 50219. doi:10.1002/app.50219

Wu, S., Deng, D., Zhou, L., Zhang, P., and Tang, G. (2019). Flame retardancy and thermal degradation of rigid polyurethane foams composites based on aluminum hypophosphite. *Mater. Res. Express* 6 (10), 105365. doi:10.1088/2053-1591/ab41b2

Xiao, X., Wang, J., Cai, D., Lou, L., and Xiao, F. (2021). A novel application of thermoplastic polyurethane/waste rubber powder blend for waterproof seal layer in high-speed railway. *Transp. Geotech.* 27, 100503. doi:10.1016/j.trgeo.2020.100503

Xiao, X., Zhai, J., Chen, T., Mai, Y., Hu, S., Ye, W., et al. (2017). Flame retardant properties of polyamide 6 with piperazine pyrophosphate. *Plast. Rubber Compos.* 46 (5), 193–199. doi:10.1080/14658011.2017.1308068

Yang, C., and Shao, S. (2021). Rigid polyurethane foams containing modified ammonium polyphosphate having outstanding charring ability and increased flame retardancy. *Front. Mat.* 8, 712809. doi:10.3389/fmats.2021.712809

Yang, Y., Dai, Z., Liu, M., Jiang, H., Fan, C., Wang, B., et al. (2021). Flame retardant rigid polyurethane foam composites based on microencapsulated ammonium polyphosphate and microencapsulated expanded graphite. *J. Macromol.Sci A* 58 (10), 659–668. doi:10.1080/10601325.2021.1920333

Yu, B., Tawiah, B., Wang, L., Yin Yuen, A. C., Zhang, Z. C., Shen, L. L., et al. (2019). Interface decoration of exfoliated MXene ultra-thin nanosheets for fire and smoke suppressions of thermoplastic polyurethane elastomer. *J. Hazard Mater*, 374:110–119. doi:10.1016/j.jhazmat.2019.04.026

Yu, B., Yuen, A., Xu, X., Zhang, Z. C., Yang, W., Lu, H., et al. (2020). Engineering MXene surface with POSS for reducing fire hazards of polystyrene with enhanced thermal stability. *J. Hazard. Mater* 401, 123342. doi:10.1016/j.jhazmat.2020.123342

Zhou, K., Gui, Z., Hu, Y., Jiang, S., and Tang, G. (2016). The influence of cobalt oxide–graphene hybrids on thermal degradation, fire hazards and mechanical properties of thermoplastic polyurethane composites. *Compos. Part A Appl. S.* 88, 10–18. doi:10.1016/j.compositesa.2016.05.014

Zhou, Q., Gong, K., Zhou, K., Zhao, S., and Shi, C. (2019). Synergistic effect between phosphorus tailings and aluminum hypophosphite in flame-retardant thermoplastic polyurethane composites. *Polym. Advan. Technol.* 30 (9), 2480–2487. doi:10.1002/pat.4695

Zhu, C., He, M., Liu, Y., Cui, J., Tai, Q., Song, L., et al. (2018). Synthesis and application of a mono-component intumescent flame retardant for polypropylene. *Polym. Degrad. Stab.* 151, 144–151. doi:10.1016/j.polymdegradstab.2018.03.007

Zhu, K. Y., Jiang, Z. L., Xu, X. T., Zhang, Y., Zhu, M., Wang, J. H., et al. (2022). Preparation and thermal cross-linking mechanism of co-polyester fiber with flame retardancy and anti-dripping by *in situ* polymerization. *RSC Adv.* 12, 168–180. doi:10.1039/D1RA07410E

Zhu, M., Zhang, Y., Sheng, H., Wang, B., and Hu, Y. (2020). Effect carbon black microencapsulated ammonium polyphosphate on the flame retardancy and mechanical properties of polyurethane composites. *Polymer-Plastics Technol. Mater.* 59 (1), 83–94. doi:10.1080/25740881.2019.1625384